Published online 10 January 2007 *Nucleic Acids Research, 2007, Vol. 35, No. 3* ***861–871***
doi:10.1093/nar/gkl1085

Tfb5 interacts with Tfb2 and facilitates nucleotide excision repair in yeast

Ying Zhou, Haiping Kou and Zhigang Wang*

Graduate Center for Toxicology, University of Kentucky, Lexington, KY 40536, USA

Received October 21, 2006; Accepted November 21, 2006

ABSTRACT

TFIIH is indispensable for nucleotide excision repair (NER) and RNA polymerase II transcription. Its tenth subunit was recently discovered in yeast as Tfb5. Unlike other TFIIH subunits, Tfb5 is not essential for cell survival. We have analyzed the role of Tfb5 in NER. NER was deficient in the *tfb5* deletion mutant cell extracts, and was specifically complemented by purified Tfb5 protein. In contrast to the extreme ultraviolet (UV) sensitivity of *rad14* mutant cells that lack any NER activity, *tfb5* deletion mutant cells were moderately sensitive to UV radiation, resembling that of the *tfb1-101* mutant cells in which TFIIH activity is compromised but not eliminated. Thus, Tfb5 protein directly participates in NER and is an accessory NER protein that stimulates the repair to the proficient level. Lacking a DNA binding activity, Tfb5 was found to interact with the core TFIIH subunit Tfb2, but not with other NER proteins. The Tfb5–Tfb2 interaction was correlated with the cellular NER function of Tfb5, supporting the functional importance of this interaction. Our results led to a model in which Tfb5 acts as an architectural stabilizer conferring structural rigidity to the core TFIIH such that the complex is maintained in its functional architecture.

INTRODUCTION

Nucleotide excision repair (NER) is a major cellular mechanism for removing DNA lesions, especially helix distorting lesions, such as *N*-acetyl-2-aminofluorene (AAF) adducts and the major ultraviolet (UV) lesions (1–7). Deficiency in NER results in human diseases xeroderma pigmentosum (XP), Cockayne's syndrome (CS) and trichothiodystrophy (TTD), depending on the specific mutations affecting various NER genes (8–10). NER consists of two sub pathways, global genome repair and transcription-coupled repair (11,12), and the repair pathways involve damage recognition, incision, excision, repair synthesis and DNA ligation.

In the yeast *Saccharomyces cerevisiae*, multiple proteins are involved in the early steps of NER, which include Rad1, Rad2, Rad4, Rad7, Rad10, Rad14, Rad16, Rad23, Rad26, Rad28, TFIIH and RPA. Rad7, Rad16, Rad26 and Rad28 are pathway-specific NER proteins in that the Rad7–Rad16 complex is specifically required for global genome repair, while Rad26 (CSB homologue) and Rad28 (CSA homologue) are specific to transcription-coupled repair (13–17). The remaining proteins are further divided into two categories: indispensable NER proteins, and accessory NER proteins. Losing any of the indispensable NER proteins results in complete inactivation of NER. In contrast, an accessory NER protein, such as Rad23 is required for full NER activity, but not all NER activity. In the absence of an accessory NER protein, some residual levels of repair remain, leading to moderate rather than severe cellular sensitivity to DNA damaging agents.

TFIIH is a large protein complex indispensable for both NER and RNA polymerase II transcription (2,18–21). The holo TFIIH is composed of two sub-complexes: core TFIIH and TFIIK (22–26). While core TFIIH is sufficient for the NER function, holo TFIIH is essential for transcription (2,18,27). For a long time, it was believed that core TFIIH consists of six subunits, Ssl2, Rad3, Tfb1, Tfb2, Ssl1 and Tfb4; and TFIIK is composed of three subunits: Tfb3, Kin28 and Ccl1 (22). Recently, Ranish *et al*. (28) identified the tenth subunit of TFIIH, named Tfb5, by quantitative proteomic analysis of RNA polymerase II preinitiation complexes. Tfb5 is believed to constitute a component of the core TFIIH complex, as it co-precipitates and co-purifies with the core TFIIH (28). However, TFB5 is in drastic contrast to the other nine subunits of TFIIH in that it is not essential for cell survival (28). Furthermore, Tfb5 is an unusually small protein of only 8 kDa. The tfb5 deletion mutant cells are sensitive to UV radiation, an indication that this protein likely plays a role in DNA repair (28). The discovery of Tfb5 led to the finding that its human homologue is encoded by the TTD-A gene (29). TTD-A cells lacking the functional TTD-A protein are known to be deficient in NER and sensitive to UV radiation (10,30). The uniqueness of Tfb5 protein raised the possibility that it may play an unusual role in TFIIH.

To better understand the Tfb5 function, we analyzed its *in vitro* and *in vivo* role in NER and examined its physical

*To whom correspondence should be addressed. Tel: +1 859 323 5784; Fax: +1 859 323 1059; Email: zwang@uky.edu

relationship with other subunits of TFIIH and NER proteins. In this report, we (i) demonstrate that Tfb5 interacts with the core TFIIH subunit Tfb2; (ii) provide evidence that the Tfb5–Tfb2 interaction is important for the NER function of Tfb5 in cells; (iii) show that Tfb5 protein directly participates in NER and (iv) reveal that Tfb5 is an accessory NER protein that stimulates the repair to the proficient level. Our results led to a model in which Tfb5 acts as an architectural stabilizer conferring structural rigidity to the core TFIIH such that the complex is maintained in the functional architecture.

MATERIALS AND METHODS

Materials

Purified yeast Tfb5 protein was obtained from Enzymax (Lexington, KY), which was purified from *Escherichia coli* cells overexpressing the yeast *TFB5* gene. Mutant Tfb5 proteins were custom-purified by Enzymax following their expression in *E.coli* cells. Protease inhibitors, alkaline phosphatase-conjugated anti-mouse IgG, 5-bromo-4-chloro-3-indolyl phosphate and nitro blue tetrazolium were obtained from Sigma Chemicals (St. Louis, MO). A mouse monoclonal antibody against the His_6 tag was purchased from Qiagen (Valencia, CA). Protein G-agarose beads were purchased from Invitrogen (Carlsbad, CA). *N*-acetoxy-*N*-2-acetylaminofluorene (AAAF, the activated form of AAF) was obtained from the Midwest Research Institute (Kansas City, MO). All oligonucleotides were synthesized by Operon (Alameda, CA). All plasmid constructs were provided by Enzymax.

S.cerevisiae strains

BY4741 (*Mata his3 leu2 met15 ura3*) was purchased from ATCC (Manassas, VA), and its isogenic *rad14* deletion mutant strain BY4741Δrad14 was purchased from Research Genetics (Huntsville, AL). BY4742 (*Matα his3 leu2 lys2 ura3*) and its isogenic *tfb5* deletion mutant strain BY4742Δtfb5 were provided by Ranish *et al*. (28). YSB207 and its isogenic *tfb1-101* strain YSB260 were obtained from Stephen Buratowski (31). Y190 (32) for the yeast two-hybrid assays was obtained from Errol C. Friedberg.

Yeast two-hybrid assays for protein interactions

Yeast Y190 cells were transformed by plasmids pAS2-TFB5 and one of the followings: pACT2-TFB1, pACT2-TFB2, pACT2-TFB3, pACT2-TFB4, pACT2-SSL1, pACT2-CCL1, pACT2-RAD3, pACT2-KIN28, pGad-SSL2, pACT2-RAD1, pACT2-RAD2, pACT2-RAD4, pACT2-RAD7, pACT2-RAD10, pACT2-RAD14, pACT2-RAD16, pACT2-RAD23, pACT2-RAD26 and pACT2-RAD28. In control experiments, the pAS2-TFB5 construct was replaced by the empty vector pAS2 for transformation. In another control experiment, cells were transformed by pAS2-Tfb5 and pACT2 or pGad. Transformed cells were grown on minimum plates for 4–6 days at 30°C. Colonies from each plate were transferred to a nitrocellulose filter and permeablized by freezing the filter in liquid nitrogen for 10 s followed by thawing at room temperature. The filter with the colony side up were placed on Whatman no. 1 paper presoaked with Z buffer (60 mM Na_2HPO_4, 40 mM NaH_2PO_4, 10 mM KCl and 1 mM $MgSO_4$) containing 38.6 mM β-mercaptoethanol and 0.5 mg/ml X-Gal. Following incubation at 30°C, cellular β-galactosidase activity was detected by the appearance of blue color in colonies derived from the colorless X-Gal. For each two-hybrid experiment, one positive control was also performed, which included the Rad6–Rad18 or the Rev1–Rev7 interaction.

Co-precipitation

For co-immunoprecipitation, protein G-agarose beads (20 μl) were washed with 1 ml of a binding buffer [0.01 M sodium phosphate (pH 7.0) and 0.15 M sodium chloride] three times and then incubated with a mouse monoclonal anti-His antibody (400 ng) at 4°C for 3 h. The agarose–protein G-antibody complex was washed with 1 ml of the binding buffer four times to remove free antibody. Purified His_6-Tfb5 protein was mixed with purified Rad3 or Tfb2 protein (2 μg each) and incubated on ice for 1.5 h. Subsequently, the protein mixture was added to the agarose–protein G-antibody complex and incubated at 4°C for another 2 h. As the control, purified His_6-Tfb5, Tfb2 or Rad3 protein was separately mixed and incubated with the agarose–protein G-antibody complex. Proteins bound to the agarose–protein G-antibody complex were collected by centrifugation and washed with 600 μl of the binding buffer six to eight times. The agarose beads containing immunoprecipitated proteins were resuspended in a buffer containing 25 mM Tris–HCl (pH 6.8), 0.05% SDS, 71.5 mM β-mercaptoethanol, 5% glycerol and 0.02% bromophenol blue. Following heating at 90–100°C for 10 min, proteins were separated by electrophoresis on a 15% SDS–polyacrylamide gel. Protein bands were identified and visualized by western blot analysis using two sequential detection steps. First, the nitrocellulose membrane containing transferred protein bands was incubated with a mouse monoclonal anti-His antibody, followed by incubation with alkaline phosphatase-conjugated anti-mouse IgG. The His_6-Tfb5 band was visualized after color development by incubating the membrane with 5-bromo-4-chloro-3-indolyl phosphate (0.3 mM) and nitroblue tetrazolium (0.4 mM) in a buffer containing 5 mM Tris–HCl (pH 7.5), 17 mM NaCl and 0.05% Tween-20. Then, Tfb2 and Rad3 proteins tagged by a calmodulin binding peptide (CBP) (33) was detected by incubating the same membrane with a detection agent (Enzymax EZ protein detector) that is specific to the tag. Color development was performed as for the His_6-Tfb5 protein described above.

For co-precipitation by calmodulin-linked agarose beads, 10 μl of calmodulin affinity resin (Stratagene, La Jolla, CA) was washed four times with 200 μl $CaCl_2$ binding buffer [50 mM Tris–HCl (pH 8.0), 150 mM NaCl, 5 mM β-mercaptoethanol, 1.0 mM magnesium acetate and 2 mM $CaCl_2$]. Purified CBP-tagged TFB2 (7 μg) was mixed with 1 μg of purified His_6-tagged TFB5 (wild-type or mutants) on ice for 1.5 h. The protein mixture was added to the equilibrated calmodulin affinity resin and incubated at 4°C for 2 h. After washing six times with $CaCl_2$ binding buffer to remove unbound protein, bound proteins were separated by electrophoresis on a 15% SDS–polyacrylamide gel. CBP-tagged TFB2 protein was identified by a detection

agent (Enzymax EZ protein detector) that is specific to the tag. Color development was achieved by incubating the membrane with 0.3 mM 5-bromo-4-chloro-3-indolyl phosphate and 0.4 mM nitroblue tetrazolium. His_6-tagged TFB5 and its mutant proteins were identified by western blot analysis using a monoclonal anti-His antibody and alkaline phosphatase- or horseradish peroxidase (HRP)-conjugated secondary antibody.

Preparation of yeast cell-free extracts

Yeast cell-free extracts were prepared essentially as described by He *et al*. (34). Briefly, yeast cells were grown at 30°C in YPD medium to an OD_{600} of ~2. Cells were harvested by centrifugation and washed once in ice-cold water and once in extraction buffer containing 0.2 M Tris–HCl (pH 7.5), 0.39 M $(NH_4)_2SO_4$, 10 mM $MgSO_4$, 1 mM EDTA, 1 mM DTT, 20% Glycerol and protease inhibitors [1 mM phenymethylsulfonyl fluoride (PMSF), 2 mM benzamidine hydrochloride, 3.5 μg/ml pepststin A, 1 μg/ml leupeptin, 0.35 μg/ml bestatin and 10 μg/ml aprotitin]. The cell pellet was scraped into a syringe, and then extruded into liquid nitrogen. The frozen cell pellets were ground to powder in liquid nitrogen using a ceramic mortar and pestle. After the liquid nitrogen was evaporated, 1 vol of cold extraction buffer was added. The mixture was transferred to a beaker and stirred for 30 min on ice. The cell lysate was centrifuged at 120 000*g* (Beckman Type 50.2 Ti rotor) for 2 h at 4°C. The clear supernatant was recovered and $(NH_4)_2SO_4$ was added to 2.94 M by adding 337 mg/ml solid $(NH_4)_2SO_4$ over the course of 1 h. After stirring for another 30 min, protein precipitates were collected by centrifugation at 40 000*g* (Beckman JA-20 rotor) for 15 min. The pellet was dissolved in a small volume (~50 μl/g of cells) of dialysis buffer containing 20 mM HEPES-KOH (pH 7.5), 10 mM $MgSO_4$, 10 mM EGTA, 5 mM DTT, 20% glycerol and protease inhibitors. The sample was dialyzed against the same buffer for 12–16 h at 4°C. Small amounts of precipitated proteins were removed by centrifugation. The resulting supernatant was collected as cell-free extract and was stored at −70°C.

In vitro NER

Plasmid pUC18 DNA containing AAF adducts was used as the repair substrate and was prepared as described previously (35). *In vitro* NER was performed as described by Wang *et al*. (1,36,37) with a slight modification. Briefly, a standard NER reaction mixture (50 μl) contained 200 ng each of damaged pUC18 DNA and undamaged pGEM3Zf DNA, 45 mM HEPES-KOH (pH 7.8), 7.4 mM $MgCl_2$, 0.9 mM DTT, 0.4 mM EDTA, 2 mM ATP, 20 μM each dATP, dGTP and dTTP, 4 μM dCTP, 1 μCi of [α-^{32}P]dCTP (3000 Ci/mmol), 40 mM phosphocreatine (disodium salt), 2.5 μg of creatine phosphokinase, 4% glycerol, 100 μg/ml BSA, 5% polyethylene glycol 8000 and 250 μg of yeast cell-free extracts. After incubation at 26°C for 2 h, EDTA and RNase A were added to 20 mM and 20 μg/ml, respectively, and incubated at 37°C for 10 min. Plasmid DNA was purified by the Wizard DNA clean-up system (Promega, Madison, WI), and linearized with the HindIII restriction endonuclease. DNA was separated by electrophoresis on a 1% agarose gel and repair synthesis was visualized by autoradiography.

Measurement of UV sensitivity

Yeast cells were grown at 30°C in YPD medium to the late log phase of growth. Appropriately diluted cells were plated onto YPD plates, and the uncovered plates were irradiated with short wave UV light from a germicidal UV lamp at the indicated doses. Surviving colonies were scored after 3–4 days of incubation in the dark at 30°C. UV survival was calculated by dividing surviving colonies after UV treatment by those without UV treatment.

For yeast strains containing a plasmid, UV sensitivity was measured with slight modifications as follows. Plasmids pEGLh6-TFB5, pEGLh6-TFB5ΔN7, pEGLh6-TFB5ΔN14, pEGLh6-TFB5ΔC7, pEGLh6-TFB5ΔC14 and the empty vector pEGLh6 were individually transformed into the *tfb5* deletion mutant strain, respectively. Yeast cells were grown at 30°C in minimum media containing 2% sucrose and the required amino acids. At an OD_{600} of ~1, protein expression from the plasmids was induced by diluting the culture 10-fold in minimum media containing 2% galactose, 0.5% sucrose and the required amino acids (YPG). After growing for 12–14 h at 30°C, cells were appropriately diluted and plated onto YPG plates. The uncovered plates were irradiated with short wave UV light at the indicated doses. Surviving colonies were scored after 3–4 days of incubation at 30°C. UV survival was calculated by dividing surviving colonies after UV treatment by those without UV treatment.

Electrophoretic mobility shift assay (EMSA)

The 79mer oligonucleotide, 5′-GGAATTCCGGAATTACAGGCTCTAACACCGAATTACAGGCTCTAACACCGTCTCATCTTCGCTCGTCCACTTTTTTTCG-3′, was 5′-labeled with T_4 polynucleotide kinase and [γ-^{32}P]ATP. To prepare duplex DNA, the labeled oligonucleotide was mixed with its complementary strand (79mer) in equal molar amounts and incubated for 5 min at 85°C in TES [10 mM Tris–HCl (pH 7.5), 1 mM EDTA and 100 mM NaCl] buffer followed by cooling slowly to room temperature. A standard DNA binding reaction mixture (10 μl) contained 50 fmol of the ^{32}P-labeled single- or double-stranded DNA, 20 mM Tris–HCl (pH 7.5), 5 mM $MgCl_2$, 1 mM DTT, 100 μg/ml BSA and a purified protein. After incubation at room temperature for 30 min, 3 μl of 50% sucrose was added. DNA was separated by electrophoresis on a 4.5% non-denaturing polyacrylamide gel at 4°C and visualized by a phosphoimager.

RESULTS

Interaction of Tfb5 with NER proteins

To gain insights into how Tfb5 might be arranged in the 10 subunit holo TFIIH, we examined physical interactions between Tfb5 and the other 9 subunits by the yeast two-hybrid assay. The yeast *TFB5* gene was cloned into the yeast two-hybrid vector pAS2 and used to determine pairwise interactions of its gene product with the other 9 subunits of TFIIH in the pACT2 vector. Positive protein–protein interaction results in activation of the reporter gene β-galactosidase in yeast cells, which turns yeast colonies blue in a filter assay in the presence of X-gal. Without interaction, the yeast colonies remain 'colorless'. Positive

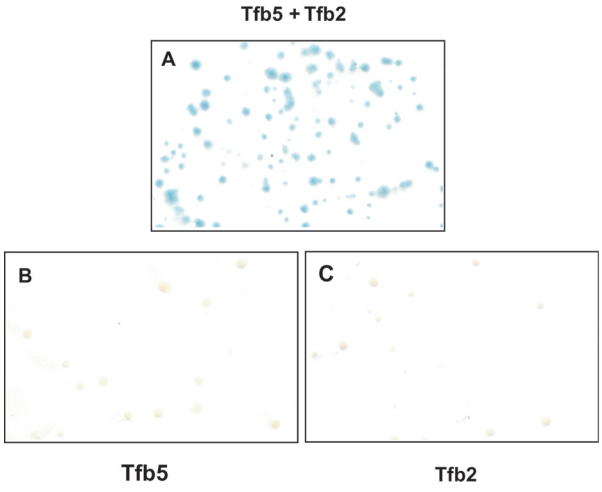

Figure 1. Interaction of Tfb5 with Tfb2. The two-hybrid vectors pAS2 and pACT2 contained the *GAL4* DNA binding domain and the *GAL4* activation domain, respectively. Yeast Y190 cells were transformed with (**A**) pAS2-TFB5 and pACT2-TFB2; (**B**) pAS2-TFB5 and pACT2; and (**C**) pAS2 and pACT2-TFB2. The expression of the two-hybrid target gene, β-galactosidase, was determined by filter assays using X-gal as the enzyme substrate. Expression of the β-galactosidase turned yeast colonies blue in the presence of X-gal, indicating physical interaction between the two proteins tested.

interaction was readily detected between Tfb5 and Tfb2 proteins (Figure 1). An interaction was not observed between Tfb5 and any of the eight remaining TFIIH subunits, Ssl2, Rad3, Tfb1, Ssl1, Tfb4, Ccl1, Tfb3 and Kin28 (data not shown). In the pACT2 vector, TFB5 gene alone activated the β-galactosidase reporter gene (data not shown), thus preventing us from performing the yeast two-hybrid assays in such an orientation.

To confirm the direct physical interaction between Tfb5 and Tfb2 proteins, we performed co-immunoprecipitation experiments using purified yeast Tfb5 and Tfb2 proteins. Tfb5 was tagged with His_6 at its N-terminus and purified to apparent homogeneity (Figure 2A). Purified yeast Tfb2 and Rad3 proteins were tagged at their *N*-termini with the CBP (33), instead of the His_6 tag. While Tfb5 was detected by western blot analysis using a mouse monoclonal antibody specific to the His_6 tag (Figure 2B, lane 2), Tfb2 and Rad3 were detected by western blot analysis using a protein detecting agent specific to the CBP (Figure 2B, lanes 3 and 4). As shown in Figure 2B (lane 5), the anti-His_6 antibody was able to precipitate the His_6-tagged Tfb5 protein. As expected, immunoprecipitation by the anti-His_6 antibody was not observed with either purified yeast Tfb2 or Rad3 protein alone (Figure 2B, lanes 6 and 7). After mixing the purified Tfb5 with Tfb2 proteins, Tfb2 was co-precipitated with Tfb5 by the anti-His_6 antibody (Figure 2B, lane 8). In contrast, the purified Rad3 could not be co-precipitated with Tfb5 by the anti-His_6 antibody (Figure 2B, lane 9). These results show that Tfb5 directly interacts with Tfb2 and suggest that Tfb5 is incorporated into the 10 subunit holo TFIIH complex through its interaction with the core subunit Tfb2.

In addition to the TFIIH complex, many Rad proteins are required in the multi-step NER pathway. Protein–protein interaction is a key mechanism in the complex process of NER. To gain insights into how Tfb5 might be engaged, if

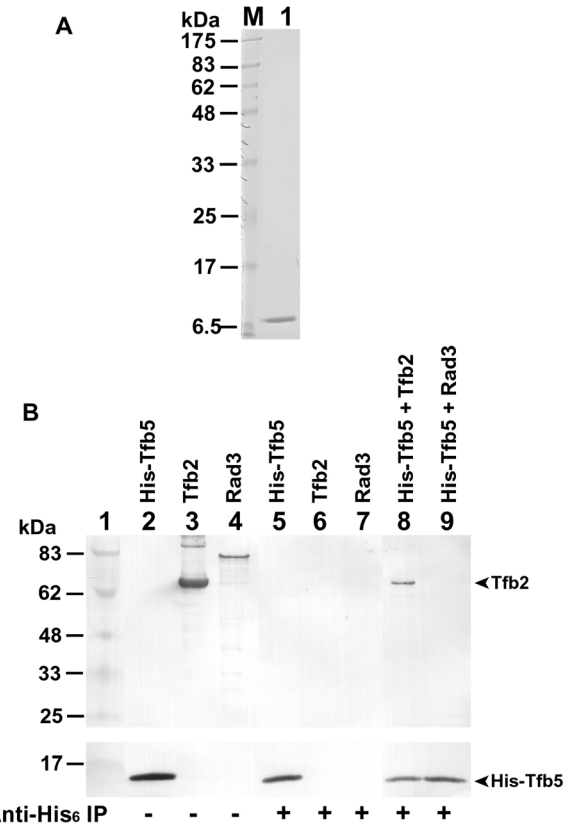

Figure 2. Co-immunoprecipitation of Tfb2 with Tfb5 protein. (**A**) Purified Tfb5 protein (430 ng) containing a His_6 tag at its N-terminus (His-Tfb5) was analyzed by electrophoresis on a 15% SDS–polyacrylamide gel and visualized by staining with Coomassie blue. The identity of the protein was confirmed by western blot analysis using a mouse monoclonal antibody specific to the His_6 tag. (**B**) Purified His-Tfb5 (lane 5), Tfb2 (lane 6), and Rad3 (lane 7) alone, or His-Tfb5 + Tfb2 (lane 8) and His-Tfb5 + Rad3 (lane 9) were precipitated with a monoclonal antibody against the His_6 tag as described in Materials and Methods. Precipitated His-Tfb5 protein was identified by western blot analysis using a monoclonal anti-His antibody. Then, the same membrane was probed again with a detection agent specific to the CBP at the N-termini of Tfb2 and Rad3. As controls, purified His_6-Tfb5 (250 ng) (lane 2), Tfb2 (350 ng) (lane 3) and Rad3 (150 ng) (lane 4) were directly loaded on to the same gel for western blot analysis. Protein markers are indicated on the left.

any, in NER, we examined physical interactions between Tfb5 and the NER Rad proteins. Pair-wise interactions were determined by the yeast two-hybrid assay. An interaction was not observed between Tfb5 and any Rad proteins examined: Rad1, Rad2, Rad4, Rad7, Rad10, Rad14, Rad16, Rad23, Rad26 and Rad28 (data not shown).

Deficient NER in *tfb5* deletion mutant cell extracts

In yeast, deleting the *TFB5* gene results in cellular sensitivity to UV radiation (28). The UV sensitive phenotype may result from defects in several different cellular processes, one of which is NER. To determine if the *TFB5* gene indeed contributes to NER, we performed *in vitro* repair assays in yeast cell-free extracts. In this assay, plasmid DNA containing AAF adducts was used as the repair substrate (Figure 3, +AAF DNA band), and another undamaged plasmid larger in size was used in the same reaction as the internal control

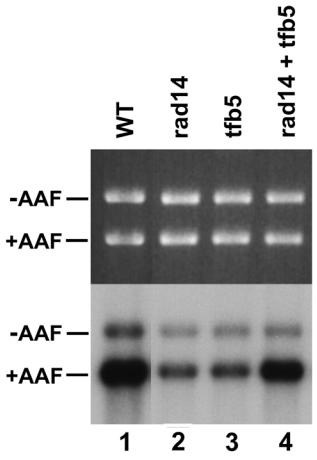

Figure 3. Deficient NER in *tfb5* deletion mutant extracts. *In vitro* NER was performed in yeast cell-free extracts (250 μg of extract protein) of the wild-type strain (WT) (lane 1), the *rad14* deletion mutant strain (lane 2), or the tfb5 deletion mutant strain (lane 3). Another *in vitro* NER assay was performed in a mixture of the *rad14* and *tfb5* mutant extracts (125 μg each) (lane 4). +AAF, AAF-damaged pUC18 DNA; −AAF, undamaged pGEM3Zf DNA as the internal control. Upper panel, ethidium bromide-stained gel; lower panel, autoradiograph of the gel.

(Figure 3, −AAF DNA band). Repair was monitored by [^{32}P]dCMP incorporation into the repair patch during repair DNA synthesis. Repair products were separated by electrophoresis on an argarose gel and visualized by autoradiography of the gel (1,38). We have previously shown that under the conditions used, AAF DNA adducts are repaired specifically by the NER pathway in yeast cell-free extracts (14,37).

Proficient *in vitro* NER results in damage-specific radio labeling of the AAF-containing plasmid in cell-free extracts of the wild-type strain, as compared to the internal control of undamaged DNA (lower panel of Figure 3, lane 1). In contrast, repair in the *rad14* deletion mutant extracts was deficient (lower panel of Figure 3, lane 2), as expected. DNA recovery from various repair reactions were similar as revealed by staining the gel with ethidium bromide (upper panel of Figure 3). As shown in Figure 3 (lane 3), *in vitro* NER in *tfb5* deletion mutant extracts was deficient. The deficient repair was complemented by *rad14* mutant extracts (Figure 3, lane 4), indicating that the tfb5 mutant extract was properly prepared and the repair deficiency was not an *in vitro* artifact. These results show that the *TFB5* gene significantly contributes to NER in yeast.

Complementation of deficient NER by purified Tfb5 protein

TFIIH functions in both NER and transcription by RNA polymerase II (2,18–21). Thus, to test the possibility that Tfb5 is directly involved in NER, we performed complementation experiments with the purified yeast Tfb5 protein. To avoid contamination by any yeast proteins, Tfb5 was expressed and purified from *E.coli* cells (Figure 2A). *In vitro* NER was deficient in the *tfb5* mutant extracts (Figure 4A, lane 1, and Figure 4B, lane 5). However, addition of the purified Tfb5 protein to the repair reaction efficiently complemented the deficient NER (Figure 4A, lanes 2–4 and Figure 4B, lane 6). The complemented NER was as efficient as repair

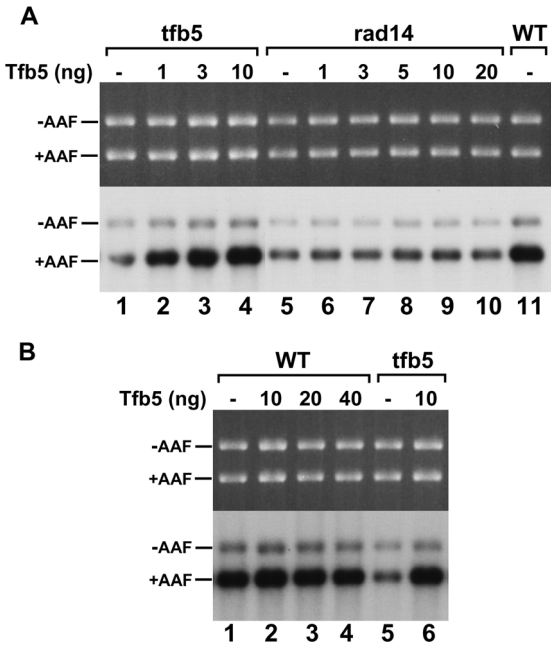

Figure 4. Specific complementation of deficient NER in *tfb5* mutant cell extracts with purified Tfb5 protein. (**A**) *In vitro* NER was performed in yeast cell-free extracts (250 μg extract protein) of the *tfb5* deletion mutant strain (lane 1), the *rad14* deletion mutant strain (lane 5), or the wild-type strain (lane 11). Complementation experiments were performed by adding increasing amounts of purified Tfb5 protein as indicated to the mutant extracts prior to the NER reactions. (**B**) *In vitro* NER was performed in yeast cell-free extracts (250 μg) of the wild-type or the *tfb5* mutant strains in the absence (lanes 1 and 5) or presence of various amounts of purified Tfb5 protein as indicated. +AAF, AAF-damaged pUC18 DNA; −AAF, undamaged pGEM3Zf DNA as the internal control. Upper, ethidium bromide-stained gel; lower, autoradiograph of the gel.

in the wild-type extracts (Figure 4A, lane 11 and Figure 4B, lane 1). As a control, purified Tfb5 had no effect on deficient repair of the *rad14* mutant extracts (Figure 4A, lanes 5–10). Adding purified Tfb5 protein to the wild-type extracts also had no effect on the proficient repair (Figure 4B, lanes 2–4), suggesting that this protein is not limiting in the wild-type yeast extracts. These results show that Tfb5 protein specifically complements the deficient NER of the tfb5 mutant extracts *in vitro*, and suggest that Tfb5 protein directly participates in the biochemistry of NER.

UV sensitivity of *tfb5* deletion mutant cells

Most NER proteins, such as Rad14, are indispensable for repair. Cells lacking any of those proteins exhibit extreme UV sensitivity. Several factors, such as Rad23, however, belong to a class of accessory NER proteins, without which NER activity is reduced but not eliminated (39,40). Cells lacking an accessory NER protein show moderate UV sensitivity. Although NER is deficient in *tfb5* deletion mutant extracts (Figures 3 and 4), the *in vitro* repair assay is not sensitive enough to allow for a clear distinction between an indispensable role versus an accessory role for Tfb5 in NER. To determine whether Tfb5 is an indispensable or accessory NER protein, we compared UV sensitivity of the *tfb5* deletion mutant strain with several other strains as an indication of *in vivo* repair capacity in the absence of Tfb5.

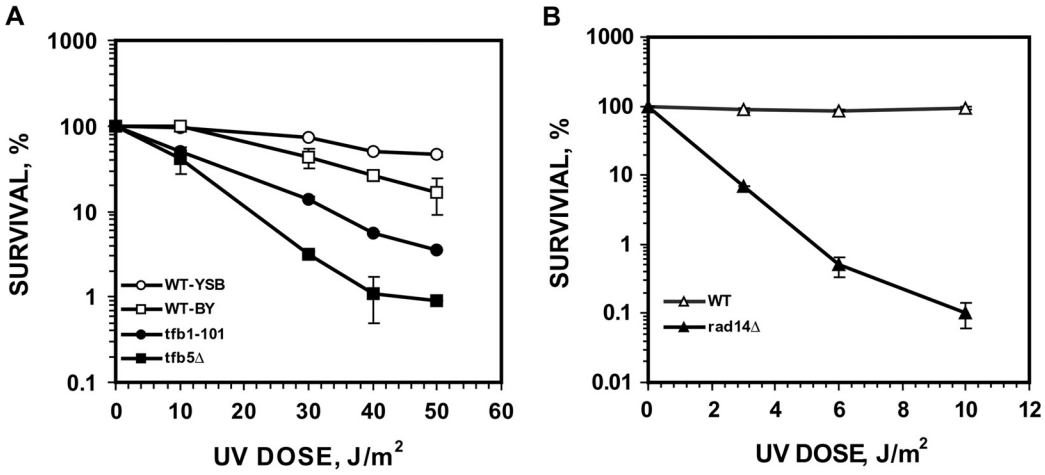

Figure 5. Comparison of UV sensitivity among various NER deficient mutant strains. Yeast cells grown in YPD media were diluted and plated onto YPD medium plates. The uncovered plates were irradiated with UV light at the indicated doses. Surviving colonies were counted after incubation at 30°C for 3–4 days. Survival rates are expressed relative to those of non-irradiated cells. Results are averages of triplicate experiments with the SDs shown as error bars. (**A**) UV sensitivity of the *tfb1-101* mutant strain (closed circle) and its isogenic wild-type strain (WT-YSB) (open circle), the *tfb5* deletion mutant strain (closed square) and its isogenic wild-type strain (WT-BY) (open square). (**B**) UV sensitivity of the *rad14* deletion mutant strain (closed triangle) and its isogenic wild-type strain (open triangle).

As reported previously by Ranish *et al*. (28), tfb5 deletion mutant cells were sensitive to UV radiation (Figure 5A). However, this sensitivity was only moderate, in contrast to the extreme UV sensitivity observed with the *rad14* deletion mutant cells (Figure 5B). For example, at a UV dose of 10 J/m^2, survivals of the wild-type, *tfb5*, and *rad14* deletion mutant cells were ~95, 42 and 0.1%, respectively.

Unlike Tfb5, the other 9 subunits of the holo TFIIH are essential for cell survival under normal growth conditions. Therefore, mutants, such as the *tfb1-101* retain partial function of TFIIH. Deficient *in vitro* repair in the *tfb1-101* mutant extracts and the moderate UV sensitivity of this strain reflect partial NER activity of these mutant cells (41). The moderate UV sensitivity of the *tfb5* deletion mutant cells resembled that of *tfb1-101* (Figure 5A), in contrast to the extreme UV sensitivity of *rad14* deletion mutant cells (Figure 5B). These results suggest that NER in the absence of Tfb5 is much reduced, but not abolished. Thus, Tfb5 is an accessory NER protein that promotes the repair rather than plays an indispensable role in the repair.

Tfb5 lacks a DNA binding activity

One possibility for Tfb5 to promote NER may be its binding to DNA at an early step during the repair. To test this possibility, we examined whether the Tfb5 protein is capable of binding to DNA by using the EMSA. A 79mer oligonucleotide labeled with ^{32}P at its 5′ end was incubated with increasing amounts of the purified Tfb5 protein. Protein binding to the DNA would retard its electrophoretic mobility on a native polyacrylamide gel. Under the conditions used, DNA binding was readily detected with the single-stranded binding (SSB) protein of the T4 bacteriophage. However, DNA binding was not observed with the purified Tfb5 protein (data not shown). Similarly, DNA binding was also not detected with Tfb5 using the double-stranded 79mer DNA (data not shown). In the control experiment, binding of the double-stranded DNA by the purified yeast PCNA was readily observed (data not shown). These results suggest that Tfb5 lacks a general DNA binding activity.

Evidence that the Tfb5–Tfb2 interaction is important for the NER function of Tfb5 in cells

To examine whether the physical interaction between Tfb5 and Tfb2 proteins is relevant to the NER function of Tfb5 in cells, we constructed several Tfb5 mutant proteins and correlated the repair function of these mutants with their ability to interact with Tfb2. The crystal structure of the human TFB5 protein (TTD-A) has been solved (deposited to the PDB database by F. Forouhar, W. Edstrom, R. Xiao, T. B. Acton, G. T. Montelione, L. Tong and J. F. Hunt). The human protein contains two helices and three β-strands (Figure 6). Sequence alignment indicates that segments corresponding to these structural elements are conserved between the yeast and the human proteins (Figure 6). Thus, the yeast Tfb5 protein likely exhibits a similar structure as its human counterpart. Accordingly, we constructed four Tfb5 mutants: Tfb5ΔN7 and Tfb5ΔN14 lacking the N-terminal 7 and 14 amino acids, respectively; Tfb5ΔC7 and Tfb5ΔC14 lacking the C-terminal 7 and 14 amino acids, respectively. Purified Tfb5 mutant proteins were examined for their ability to interact with pure Tfb2 protein using a co-precipitation method. Tfb2 protein was tagged at its N-terminus with a CBP and thus effectively precipitated by calmodulin-conjugated agarose beads (Figure 7A, lane 2). Like the wild-type Tfb5 (Figure 7A, lane 4), Tfb5ΔN7 and Tfb5ΔC14 mutant proteins were specifically co-precipitated with Tfb2 (Figure 7A, lanes 5–8). Interaction between Tfb5ΔC7 and Tfb2 was revealed by the yeast two-hybrid assay (data not shown). The N-terminal Tfb5 deletion mutants alone activated the β-galactosidase reporter gene in either the pAS2 or the pACT2 two-hybrid vector (data not show), thus preventing us from performing interaction experiments with these mutant proteins by the yeast two-hybrid assay. These results show that Tfb5ΔN7, Tfb5ΔC7

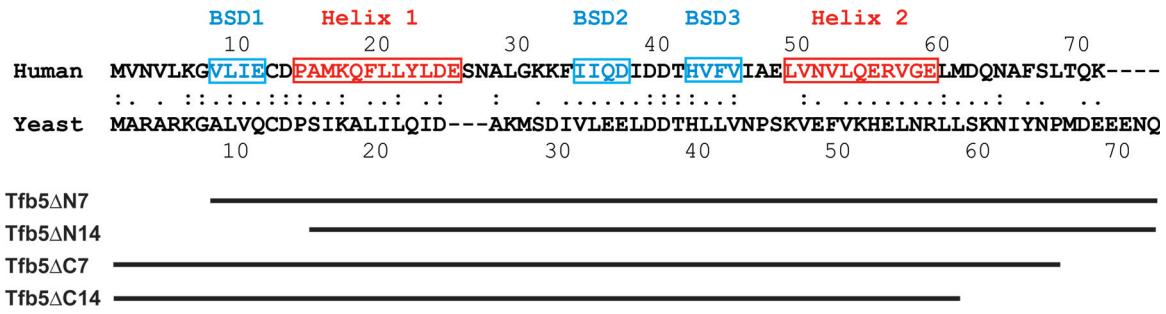

Figure 6. Schematic presentation of the Tfb5 mutant proteins constructed. The complete amino acid sequences of the human and the yeast Tfb5 proteins were aligned with identical amino acids indicated by two dots and conservative substitutions indicated by a single dot between the two sequences. Features of the secondary structure is from the crystal structure of the human TFB5 protein (TTD-A), which was deposited to the PDB database by F. Forouhar, W. Edstrom, R. Xiao, T. B. Acton, G. T. Montelione, L. Tong and J. F. Hunt. BSD, β-strand.

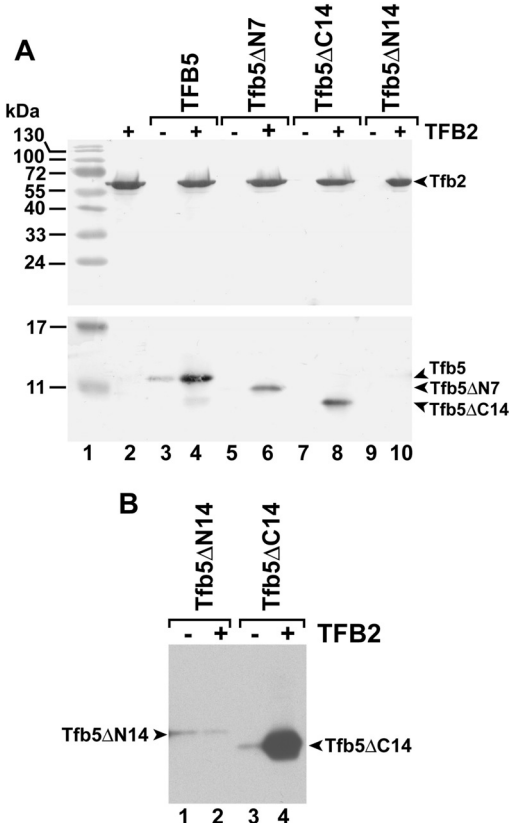

Figure 7. Co-precipitation of Tfb5 mutant proteins with Tfb2. (**A**) Purified Tfb5 (lane 3), Tfb5ΔN7 (lane 5), Tfb5ΔC14 (lane 7) and Tfb5ΔN14 (lane 9) alone (1 μg each) or in the presence of purified Tfb2 protein (7 μg) (lanes 4, 6, 8 and 10) were precipitated with calmodulin-linked agarose beads as described in Materials and Methods. While Tfb5 and its mutant proteins were tagged at their N-termini by His_6, Tfb2 protein was tagged at its N-terminus by a CBP. Thus, the precipitation targeted Tfb2 (lane 1). Precipitated Tfb2 protein was identified by a detection agent specific to the CBP in a western blot analysis. Co-precipitated Tfb5 and its mutant proteins were identified by western blot analysis using a monoclonal anti-His antibody. Protein markers are indicated on the left. (**B**) Co-precipitation experiments were performed as in (A) except that the Tfb5 mutant proteins were identified by a more sensitive method of HRP-mediated bioluminescence during western blot analysis.

and Tfb5ΔC14 mutant proteins retain the ability to interact with Tfb2 protein.

In contrast, Tfb5ΔN14 could not be co-precipitated with Tfb2 (Figure 7A, lanes 9 and 10). To exclude the possibility that this negative result might result from reduced sensitivity of the His_6-tagged Tfb5ΔN14 protein to the anti-His monoclonal antibody during western blotting, we performed the co-precipitation experiment again using the more sensitive detection method of HRP-linked secondary antibody for western blotting. The detection was so sensitive that a faint Tfb5ΔC14 band non-specifically precipitated in the absence of Tfb2 protein was observed (Figure 7B, lane 3). With the Tfb5ΔN14 co-precipitation experiment, only a non-specifically precipitated faint band (Tfb5ΔN14) was detected in the absence or presence of Tfb2 (Figure 7B, lanes 1 and 2). Therefore, the Tfb5ΔN14 mutant protein is unable to interact with Tfb2 protein.

To determine the NER function of these mutant Tfb5 proteins in yeast cells, we expressed each mutant protein from a plasmid in the *tfb5* deletion mutant strain and measured UV sensitivity of these transformed cells. As shown in Figure 8, UV sensitivity of the wild-type cells was not affected by transformation with either the empty vector or the wild-type *TFB5* gene. The *tfb5* deletion mutant cells remained sensitive to UV radiation when transformed by the empty vector, and were fully complemented by transformation of the wild-type *TFB5* gene, as expected. UV sensitivity of the mutant cells were also complemented by the mutant proteins Tfb5ΔN7, Tfb5ΔC7 and Tfb5ΔC14, respectively. In contrast, the Tfb5ΔN14 mutant protein was unable to complement the UV sensitivity of the *tfb5* deletion mutant cells. These results show that whereas the Tfb5ΔN7, Tfb5ΔC7 and Tfb5ΔC14 mutant proteins are proficient for NER, the Tfb5ΔN14 mutant protein has lost its NER function in cells.

Taken together, these results correlate the Tfb5–Tfb2 interaction with the cellular NER function of Tfb5. Deleting the C-terminal 14 amino acids of Tfb5 did not significantly affect its interaction with Tfb2 and its NER function. On the other hand, deleting the N-terminal region of Tfb5 by only 14 amino acids abolished its interaction with Tfb2. Consequently, the NER activity of Tfb5 was inactivated. Thus, these results suggest that the Tfb5–Tfb2 interaction is important for the NER function of Tfb5 in yeast cells.

DISCUSSION

In this study, we examined the role of Tfb5 protein in yeast NER by two approaches: its physical interaction with

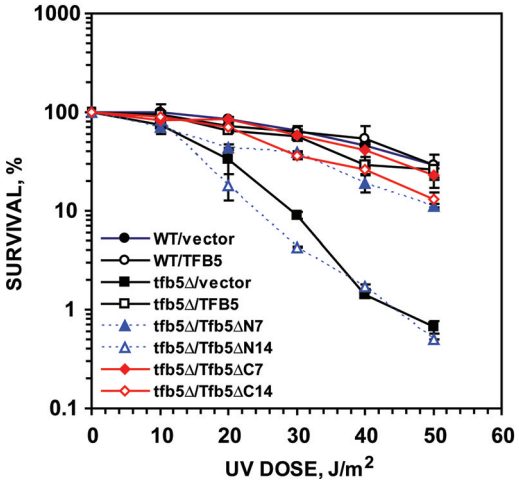

Figure 8. Complementation of UV sensitivity of the *tfb5* deletion mutant cells by various Tfb5 mutant proteins. Yeast cells containing the empty plasmid vector or expressing various mutant Tfb5 mutant proteins from a plasmid were diluted and plated onto YPG minimal medium plates as described in Materials and Methods. The uncovered plates were irradiated with UV light at the indicated doses. Surviving colonies were counted after incubation at 30°C for 3–4 days. Survival rates are expressed relative to those of non-irradiated cells. Results are averages of duplicate experiments with the SDs shown as error bars. Closed circle, wild-type strain containing the empty vector; open circle, wild-type strain expressing the wild-type Tfb5 protein from the plasmid; closed square, *tfb5* deletion mutant strain containing the empty vector; open square, *tfb5* deletion mutant strain complemented by the wild-type Tfb5 protein; closed triangle, *tfb5* deletion mutant strain complemented by Tfb5ΔN7; open triangle, *tfb5* deletion mutant strain complemented by Tfb5ΔN14; closed diamond, *tfb5* deletion mutant strain complemented by Tfb5ΔC7; open diamond, *tfb5* deletion mutant strain complemented by Tfb5ΔC14.

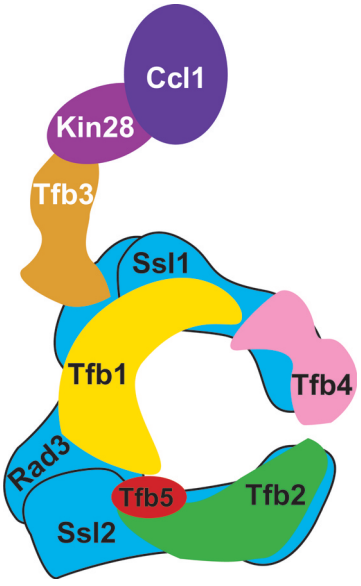

Figure 9. A model of the yeast TFIIH complex. A ring structure is formed by Ssl1, Rad3 and Ssl2, on which another layer of ring structure is formed by Tfb1, Tfb2 and Tfb4 through Ssl1–Tfb1, Ssl1–Tfb4 and Ssl2–Tfb2 interactions. However, Tfb1, Tfb2 and Tfb4 do not interact with each other, resulting in a fragile layer of ring structure. This fragile 6 subunit core TFIIH is stabilized by fitting the small Tfb5 into the structure through the Tfb5–Tfb2 interaction. Tfb5 may also help locking Tfb1 in place in the core TFIIH ring structure. Thus, the Tfb5 protein uniquely serves as the architectural stabilizer of the core TFIIH. The TFIIK sub-complex consisting of Tfb3, Kin28 and Ccl1 is assembled onto the core TFIIH through the Tfb3–Rad3 interaction, forming the 10 subunit holo TFIIH.

NER proteins and its contribution to *in vitro* and *in vivo* repair. We found that Tfb5 protein physically interacts with Tfb2 and directly participates in NER. However, NER is largely but not completely dependent on Tfb5. In the absence of Tfb5, NER becomes rather inefficient, but is not eliminated. Our results suggest that Tfb5 functions as an accessory NER protein to facilitate efficient repair. This facilitating role of Tfb5 is reminiscent of the role of Rad23 in NER (35,40).

Based on the observation that Tfb5 co-precipitates and co-purifies with the core TFIIH, Ranish *et al*. (28) concluded that Tfb5 is a component of the core TFIIH. The core TFIIH is indispensable for both transcription and NER (2,18–21). In contrast, the TFIIK of the holo TFIIH, which consists of Tfb3, Kin28 and Ccl1, is not required for NER (18,27). Our results extend the studies of Ranish *et al*. (28) by showing that Tfb5 is incorporated into the core TFIIH sub-complex through its interaction with Tfb2. Moreover, our results that Tfb5 plays an important role in NER indicate that Tfb5 is indeed both a structural and functional component of the core TFIIH. Among the 10 subunit holo TFIIH, the following physical interactions are known: Ssl1-Rad3, Ssl1-Tfb1, Ssl1-Tfb4, Rad3-Ssl2, Ssl2-Tfb2, Rad3-Tfb3, Tfb3-Kin28, Kin28-Ccl1 (20,31,42–45) and Tfb2-Tfb5 (this study). Low-resolution electron microscopic structures of TFIIH crystals were also reported (46,47). Based on these reports and the Tfb5–Tfb2 interaction of this study, a model of the holo TFIIH is depicted in Figure 9.

As a component of TFIIH, Tfb5 is unique in that it is not essential for cell survival under normal growth conditions. Thus, the contribution of Tfb5 protein to NER can be definitively determined by using the *tfb5* deletion mutant cells. *In vitro* biochemical experiments demonstrated that Tfb5 is an NER protein. Its role in repair, however, is intriguing as revealed by the UV sensitivity experiments. Deleting the *TFB5* gene results in moderate rather than extreme UV sensitivity. Quantitative comparison of UV sensitivity suggests that cells retain some NER activity in the absence of the Tfb5 protein, a situation similar to when TFIIH is only partially functional. Consistent with such a partial or inefficient TFIIH function in repair, tfb5 deletion mutant cells also exhibit a slow growth phenotype, indicating that the transcription activity of TFIIH is not fully functional in the absence of the Tfb5 protein (28). Thus, whereas the core TFIIH and six of its subunits, Ssl2, Rad3, Tfb1, Tfb2, Ssl1 and Tfb4, are essential for both transcription and repair, Tfb5 plays an accessory role for both transcription and repair as the seventh subunit of the core TFIIH. This functionally sets Tfb5 apart from the other 6 subunits of the essential core TFIIH factor.

What is the molecular role of the Tfb5 protein in NER? One possibility might be an indirect role for Tfb5 by maintaining adequate transcription of one or more NER genes. We have excluded this possibility by showing that the purified Tfb5 protein alone is sufficient to complement the deficient NER of the *tfb5* deletion mutant extracts. That is, without the Tfb5 protein, other NER proteins are present in sufficient quantities. Hence, the Tfb5 protein directly

functions in the biochemistry of the NER pathway. Then, how does the Tfb5 protein act in the biochemistry of the repair? Since TFIIH acts between damage recognition and DNA incisions, this protein complex is recruited and is likely involved in recruiting other NER proteins to the lesion site through protein–protein interactions. Indeed, physical interactions, such as Rad2-Tfb1 and Rad2-Ssl2 have been observed (48). Thus, we examined Tfb5 interaction with other NER proteins by the yeast two-hybrid assay. However, we did not observe an interaction between Tfb5 and any of these NER proteins: Rad1, Rad2, Rad4, Rad7, Rad10, Rad14, Rad16, Rad23, Rad26 and Rad28. Another important activity during repair is DNA binding. Again, we did not observe a Tfb5 binding activity to either single-stranded or double-stranded DNA.

We propose that Tfb5 functions as an architectural stabilizer to maintain the proper architecture of the core TFIIH complex. The properly structured 6 subunit core TFIIH consisting of Ssl2, Rad3, Tfb1, Tfb2, Ssl1 and Tfb4 would be sufficient to attain its biochemical activity in repair and transcription. However, without the small Tfb5 protein, the core TFIIH complex would become fragile and prone to collapse. Thus, in the *tfb5* deletion mutant cells, whereas some core TFIIH complexes remain functional, a fraction of them would lose activity due to architectural collapse of the complex. This would explain the phenotype of partial TFIIH function in transcription and repair for these mutant cells. Adding purified Tfb5 protein to the mutant extracts would restore the collapsed core TFIIH complexes, leading to *in vitro* complementation of the deficient NER. Reminiscent of Tfb5, another accessory NER protein is Rad23. However, Rad23 plays two different roles in NER: preventing Rad4 protein degradation by the protesome system (35,49–51); and directly stimulating repair (35).

Tfb5 is evolutionarily conserved in eukaryotes. Its human homologue is the TTD-A protein (29). Inactivating mutations have been found in TTD-A patient cells, indicating that it is not essential for cellular growth like its yeast counterpart (9,10,29). Inherited loss of TTD-A in humans results in the hereditary disease TTD, a complex disease showing clinical symptoms that include photosensitivity, ichthyosis (scaly skin), brittle hair, impaired intelligence, decreased fertility and short stature (9,10). Clinical manifestations of the TTD-A disease and phenotypes of the yeast *tfb5* deletion mutant cells share the common functional defects: insufficient TFIIH activity leading to deficiencies in both NER and transcription (9,10,28,29) (this study). Therefore, our architectural stabilizer model for Tfb5 may be extrapolated to the human TTD-A protein, which is able to explain the cellular and clinical consequences of the TTD-A disease in a similar way as we explained the phenotypes of the yeast *tfb5* deletion mutant cells. Indeed, the Tfb5–Tfb2 interaction was also observed recently in the human system between TTD-A and p52 (the Tfb2 homologue) (52). Thus, the Tfb5–Tfb2 interaction is conserved from yeast to humans, consistent with our conclusion that this interaction is functionally important. A difference, however, is noted. In yeast, deleting the TFB5 gene does not alter cellular concentrations of other TFIIH components, as demonstrated by western blot analyses of the Tfb1 and Kin28 subunits (28) and our results that Tfb5 protein alone is sufficient to complement deficient NER in the mutant extracts. In human TTD-A mutant cells, it was reported that the steady-state level of TFIIH is reduced (53). We speculate that architectural collapse of some core TFIIH complexes in the absence of TTD-A protein may lead to degradation of the individual subunits in mammalian cells.

Our studies led to the model that 9 subunits form a large and functional, but fragile protein complex, the holo TFIIH, which requires the tenth subunit, Tfb5/TTD-A, to stabilize its elegant architecture, in order to attain its full cellular proficiency in transcription and repair. Such a role of architectural stabilizer is a unique and novel mechanism in the NER pathway. As an architectural stabilizer, the Tfb5/TTD-A protein needs to be stable/non-fragile itself, which would be best served by a small instead of a large protein. This is consistent with the fact that Tfb5/TTD-A is the smallest NER protein (~8 kDa), an unusually small protein even among all types of DNA repair systems.

ACKNOWLEDGEMENTS

The authors thank Jeffrey A. Ranish for the yeast *tfb5* deletion mutant and its isogenic wild-type strains, Stephen Buratowski for the *tfb1-101* mutant and its isogenic wild-type strains and Errol C. Friedberg for the yeast Y190 strain and plasmid vectors pAS2 and pACT2. This work was supported by the NIH grant CA67978. Funding to pay the Open Access publication charges for this article was provided by the NIH grant CA67978.

Conflict of interest statement. None declared.

REFERENCES

1. Wang,Z., Wu,X. and Friedberg,E.C. (1993) Nucleotide-excision repair of DNA in cell-free extracts of the yeast *Saccharomyces cerevisiae*. *Proc. Natl Acad. Sci. USA*, **90**, 4907–4911.
2. Wang,Z., Svejstrup,J.Q., Feaver,W.J., Wu,X., Kornberg,R.D. and Friedberg,E.C. (1994) Transcription factor b (TFIIH) is required during nucleotide-excision repair in yeast. *Nature*, **368**, 74–76.
3. Braithwaite,E., Wu,X. and Wang,Z. (1998) Repair of DNA lesions induced by polycyclic aromatic hydrocarbons in human cell-free extracts: involvement of two excision repair mechanisms *in vitro*. *Carcinogenesis*, **19**, 1239–1246.
4. Braithwaite,E., Wu,X. and Wang,Z. (1999) Repair of DNA lesions: mechanisms and relative repair efficiencies. *Mutat. Res.*, **424**, 207–219.
5. Aboussekhra,A., Biggerstaff,M., Shivji,M.K.K., Vilpo,J.A., Moncollin,V., Podust,V.N., Protic,M., Hubscher,U., Egly,J.-M. and Wood,R.D. (1995) Mammalian DNA nucleotide excision repair reconstituted with purified protein components. *Cell*, **80**, 859–868.
6. Huang,J.C., Svoboda,D.L., Reardon,J.T. and Sancar,A. (1992) Human nucleotide excision nuclease removes thymine dimers from DNA by incising the 22nd phosphodiester bond 5′ and the 6th phosphodiester bond 3′ to the photodimer. *Proc. Natl Acad. Sci. USA*, **89**, 3664–3668.
7. Kusumoto,R., Masutani,C., Sugasawa,K., Iwai,S., Araki,M., Uchida,A., Mizukoshi,T. and Hanaoka,F. (2001) Diversity of the damage recognition step in the global genomic nucleotide excision repair *in vitro*. *Mutat. Res.*, **485**, 219–227.
8. Cleaver,J.E. and Kraemer,K.H. (1989) Xeroderma pigmentosum. In Scriver,C.R., Beaudet,A.L., Sly,W.S. and Valle,D. (eds), *The Metabolic Basis of Inherited Disease*, *6th edn*. McGraw-Hill Book Co., NY, pp. 2949–2971.
9. Lehmann,A.R. (2001) The xeroderma pigmentosum group D (XPD) gene: one gene, two functions, three diseases. *Genes Dev.*, **15**, 15–23.
10. de Boer,J. and Hoeijmakers,J.H. (2000) Nucleotide excision repair and human syndromes. *Carcinogenesis*, **21**, 453–460.

11. Hanawalt,P.C. (1994) Transcription-coupled repair and human disease. *Science*, **266**, 1957–1958.
12. de Laat,W.L., Jaspers,N.G. and Hoeijmakers,J.H. (1999) Molecular mechanism of nucleotide excision repair. *Genes Dev.*, **13**, 768–785.
13. Verhage,R., Zeeman,A.-M., Gleig,F., Bang,D.D., van de Putte,P. and Brouwer,J. (1994) The *RAD7* and *RAD16* genes, which are essential for pyrimidine dimer removal from the silent mating type loci, are also required for repair of the nontranscribed strand of an active gene in *Saccharomyces cerevisiae*. *Mol. Cell. Biol.*, **14**, 6135–6142.
14. Wang,Z., Wei,S., Reed,S.H., Wu,X., Svejstrup,J.Q., Feaver,W.J., Kornberg,R.D. and Friedberg,E.C. (1997) The *RAD7*, *RAD16* and *RAD23* genes of *S. cerevisiae*: requirement for transcription-independent nucleotide excision repair *in vitro* and interactions between the gene products. *Mol. Cell. Biol.*, **17**, 635–643.
15. Verhage,R.A., van Gool,A.J., de Groot,N., Hoeijmakers,J.H., van de Putte,P. and Brouwer,J. (1996) Double mutants of *Saccharomyces cerevisiae* with alterations in global genome and transcription-coupled repair. *Mol. Cell. Biol.*, **16**, 496–502.
16. van Gool,A.J., Verhage,R., Swagemakers,S.M.A., van de Putte,P., Brouwer,J., Troelstra,C., Bootsma,D. and Hoeijmakers,J.H.J. (1994) RAD26, the functional *S. cerevisiae* homolog of the Cockayne syndrome B gene *ERCC6*. *EMBO J.*, **13**, 5361–5369.
17. Bhatia,P.K., Verhage,R.A., Brouwer,J. and Friedberg,E.C. (1996) Molecular cloning and characterization of *Saccharomyces cerevisiae RAD28*, the yeast homolog of the human Cockayne syndrome A (CSA) gene. *J. Bacteriol.*, **178**, 5977–5988.
18. Araujo,S.J., Tirode,F., Coin,F., Pospiech,H., Syvaoja,J.E., Stucki,M., Hubscher,U., Egly,J.M. and Wood,R.D. (2000) Nucleotide excision repair of DNA with recombinant human proteins: definition of the minimal set of factors, active forms of TFIIH, and modulation by CAK. *Genes Dev.*, **14**, 349–359.
19. Schaeffer,L., Roy,R., Humbert,S., Moncollin,V., Vermeulen,W., Hoeijmakers,J.H.J., Chambon,P. and Egly,J.-M. (1993) DNA repair helicase: a component of BTF2 (TFIIH) basic transcription factor. *Science*, **260**, 58–63.
20. Feaver,W.J., Svejstrup,J.Q., Bardwell,L., Bardwell,A.J., Buratowski,S., Gulyas,K.D., Donahue,T.F., Friedberg,E.C. and Kornberg,R.D. (1993) Dual roles of a multiprotein complex from *S. cerevisiae* in transcription and DNA repair. *Cell*, **75**, 1379–1387.
21. Svejstrup,J.Q., Feaver,W.J., LaPointe,J. and Kornberg,R.D. (1994) RNA polymerase transcription factor IIH holoenzyme from yeast. *J. Biol. Chem.*, **269**, 28044–28048.
22. Takagi,Y., Komori,H., Chang,W.H., Hudmon,A., Erdjument-Bromage,H., Tempst,P. and Kornberg,R.D. (2003) Revised subunit structure of yeast transcription factor IIH (TFIIH) and reconciliation with human TFIIH. *J. Biol. Chem.*, **278**, 43897–43900.
23. Roy,R., Adamczewski,J.P., Seroz,T., Vermeulen,W., Tassan,J.-P., Schaeffer,L., Nigg,E.A., Hoeijmakers,J.H.J. and Egly,J.-M. (1994) The MO15 cell cycle kinase is associated with the TFIIH transcription-DNA repair factor. *Cell*, **79**, 1093–1101.
24. Feaver,W.J., Svejstrup,J.Q., Henry,N.L. and Kornberg,R.D. (1994) Relationship of CDK-activating kinase and RNA polymerase II CTD kinase TFIIH/TFIIK. *Cell*, **79**, 1103–1109.
25. Shiekhattar,R., Mermelstein,F., Fisher,R.P., Drapkin,R., Dynlacht,B., Wesling,H.C., Morgan,D.O. and Reinberg,D. (1995) Cdk-activating kinase complex is a component of human transcription factor TFIIH. *Nature*, **374**, 283–287.
26. Serizawa,H., Makela,T.P., Conaway,J.W., Conaway,R.C., Weinberg,R.A. and Young,R.A. (1995) Association of Cdk-activating kinase subunits with transcription factor THIIH. *Nature*, **374**, 280–282.
27. Svejstrup,J.Q., Wang,Z., Feaver,W.J., Wu,X., Bushnell,D.A., Donahue,T.F., Friedberg,E.C. and Kornberg,R.D. (1995) Different forms of TFIIH for transcription and DNA repair: holo-TFIIH and a nucleotide excision repairosome. *Cell*, **80**, 21–28.
28. Ranish,J.A., Hahn,S., Lu,Y., Yi,E.C., Li,X.J., Eng,J. and Aebersold,R. (2004) Identification of TFB5, a new component of general transcription and DNA repair factor IIH. *Nature Genet.*, **36**, 707–713.
29. Giglia-Mari,G., Coin,F., Ranish,J.A., Hoogstraten,D., Theil,A., Wijgers,N., Jaspers,N.G., Raams,A., Argentini,M., van der Spek,P.J. *et al.* (2004) A new, tenth subunit of TFIIH is responsible for the DNA repair syndrome trichothiodystrophy group A. *Nature Genet.*, **36**, 714–719.
30. Stefanini,M., Vermeulen,W., Weeda,G., Giliani,S., Nardo,T., Mezzina,M., Sarasin,A., Harper,J.I., Arlett,C.F., Hoeijmakers,J.H.J. *et al.* (1993) A new nucleotide-excision-repair gene associated with the disorder trichothiodystrophy. *Am. J. Hum. Genet.*, **53**, 817–821.
31. Matsui,P., DePaulo,J. and Buratowski,S. (1995) An interaction between the Tfb1 and Ssl1 subunits of yeast TFIIH correlates with DNA repair activity. *Nucleic Acids Res.*, **23**, 767–772.
32. Bai,C. and Elledge,S.J. (1996) Gene identification using the yeast two-hybrid system. *Meth. Enzymol.*, **273**, 331–347.
33. Stofko-Hahn,R.E., Carr,D.W. and Scott,J.D. (1992) A single step purification for recombinant proteins. Characterization of a microtubule associated protein (MAP 2) fragment which associates with the type II cAMP-dependent protein kinase. *FEBS Lett.*, **302**, 274–278.
34. He,Z., Wong,J.M.S., Maniar,H.S., Brill,S.J. and Ingles,C.J. (1996) Assessing the requirements for nucleotide excision repair proteins of *Saccharomyces cerevisiae* in an *in vitro* system. *J. Biol. Chem.*, **271**, 28243–28249.
35. Xie,Z., Liu,S., Zhang,Y. and Wang,Z. (2004) Roles of Rad23 protein in yeast nucleotide excision repair. *Nucleic Acids Res.*, **32**, 5981–5990.
36. Wang,Z., Wu,X. and Friedberg,E.C. (1992) Excision repair of DNA in nuclear extracts from the yeast *Saccharomyces cerevisiae*. *Biochemistry*, **31**, 3694–3702.
37. Wang,Z., Wu,X. and Friedberg,E.C. (1996) A yeast whole cell extract supports nucleotide excision repair and RNA polymerase II transcription *in vitro*. *Mutat. Res.*, **364**, 33–41.
38. Wood,R.D., Robins,P. and Lindahl,T. (1988) Complementation of the Xeroderma pigmentosum DNA repair defect in cell-free extracts. *Cell*, **53**, 97–106.
39. Watkins,J.F., Sung,P., Prakash,L. and Prakash,S. (1993) The *Saccharomyces cerevisiae* DNA repair gene RAD23 encodes a nuclear protein containing a ubiquitin-like domain required for biological function. *Mol. Cell. Biol.*, **13**, 7757–7773.
40. Mueller,J.P. and Smerdon,M.J. (1996) Rad23 is required for transcription-coupled repair and efficient overrall repair in *Saccharomyces cerevisiae*. *Mol. Cell. Biol.*, **16**, 2361–2368.
41. Wang,Z., Buratowski,S., Svejstrup,J.Q., Feaver,W.J., Wu,X., Kornberg,R.D., Donahue,T.F. and Friedberg,E.C. (1995) Yeast *TFB1* and *SSL1* genes, which encode subunits of transcription factor IIH, are required for nucleotide excision repair and RNA polymerase II transcription. *Mol. Cell. Biol.*, **15**, 2288–2293.
42. Bardwell,L., Bardwell,A.J., Feaver,W.J., Svejstrup,J.Q., Kornberg,R.D. and Friedberg,E.C. (1994) Yeast RAD3 protein binds directly to both SSL2 and SSL1 proteins: implications for the structure and function of transcription/repair factor b. *Proc. Natl Acad. Sci. USA*, **91**, 3926–3930.
43. Feaver,W.J., Henry,N.L., Wang,Z., Wu,X., Svejstrup,J.Q., Bushnell,D.A., Friedberg,E.C. and Kornberg,R.D. (1997) Genes for Tfb2, Tfb3, and Tfb4 subunits of yeast transcription/repair factor IIH. Homology to human cyclin-dependent kinase activating kinase and IIH subunits. *J. Biol. Chem.*, **272**, 19319–19327.
44. Valay,J.G., Simon,M. and Faye,G. (1993) The Kin28 protein kinase is associated with a cyclin in *Saccharomyces cerevisiae*. *J. Mol. Biol.*, **234**, 307–310.
45. Feaver,W.J., Huang,W., Gileadi,O., Myers,L., Gustafsson,C.M., Kornberg,R.D. and Friedberg,E.C. (2000) Subunit interactions in yeast transcription/repair factor TFIIH. Requirement for Tfb3 subunit in nucleotide excision repair. *J. Biol. Chem.*, **275**, 5941–5946.
46. Chang,W.H. and Kornberg,R.D. (2000) Electron crystal structure of the transcription factor and DNA repair complex, core TFIIH. *Cell*, **102**, 609–613.
47. Schultz,P., Fribourg,S., Poterszman,A., Mallouh,V., Moras,D. and Egly,J.M. (2000) Molecular structure of human TFIIH. *Cell*, **102**, 599–607.
48. Bardwell,A.J., Bardwell,L., Iyer,N., Svejstrup,J.Q., Feaver,W.J., Kornberg,R. and Friedberg,E.C. (1994) Yeast nucleotide excision

repair proteins Rad2 and Rad4 interact with RNA polymerase II basal transcription factor b (TFIIH). *Mol. Cell. Biol.*, **14**, 3569–3576.
49. Lommel,L., Ortolan,T., Chen,L., Madura,K. and Sweder,K.S. (2002) Proteolysis of a nucleotide excision repair protein by the 26 S proteasome. *Curr. Genet.*, **42**, 9–20.
50. Ng,J.M., Vermeulen,W., van der Horst,G.T., Bergink,S., Sugasawa,K., Vrieling,H. and Hoeijmakers,J.H. (2003) A novel regulation mechanism of DNA repair by damage-induced and RAD23-dependent stabilization of xeroderma pigmentosum group C protein. *Genes Dev.*, **17**, 1630–1645.
51. Ortolan,T.G., Chen,L., Tongaonkar,P. and Madura,K. (2004) Rad23 stabilizes Rad4 from degradation by the Ub/proteasome pathway. *Nucleic Acids Res.*, **32**, 6490–6500.
52. Coin,F., Proietti De Santis,L., Nardo,T., Zlobinskaya,O., Stefanini,M. and Egly,J.M. (2006) p8/TTD-A as a repair-specific TFIIH subunit. *Mol. Cell*, **21**, 215–226.
53. Vermeulen,W., Bergmann,E., Auriol,J., Rademakers,S., Frit,P., Appeldoorn,E., Hoeijmakers,J.H. and Egly,J.M. (2000) Sublimiting concentration of TFIIH transcription/DNA repair factor causes TTD-A trichothiodystrophy disorder. *Nature Genet.*, **26**, 307–313.